AIAA'84

AIAA-84-2163

On the Aerodynamic Optimization of Mini-RPV and Small GA Aircraft

F. R. Goldschmied, Monroeville, PA

AIAA 2nd Applied Aerodynamics Conference

August 21-23, 1984/Seattle, Washington

ON THE AERODYNAMIC OPTIMIZATION OF MINI-RPV AND SMALL GA AIRCRAFT

Fabio R. Goldschmied*
Monroeville, PA 15146

Abstract

A brief study has been carried out on the adaptation of an optimized system comprising an axisymmetric body, suction boundary-layer control and stern jet-propulsion, which was developed originally for lighter-than-air application, to mini-RPV and small GA aircraft by the addition of dynamic wing lift. For mini-RPV, consideration has been given to fuselage diameters of 20 and 34" with a gross weight range from 125 to 300 lb at the speeds of 100 and 150 Kn. The predicted powers ranged from 2.35 to 16.20 HP.

For the GA aircraft, consideration has been given to fuselage diameters of 45 and 60" with a gross weight range from 1400 to 3400 lb at the speed of 200 MPH. The predicted powers ranged from 60.6 to 132.5 HP.

Nomenclature

A	Wing area, ft^2
AR	Aspect ratio
B	Wing span, ft
C	Wing chord, ft
$C_D = \frac{F_w}{q_o A}$	Wing drag coefficient
$CH_{25} = \frac{\Delta H_{25}}{q_o}$	*Fan pressure-rise coefficient*
$CHP_{25} = \frac{Q\Delta H_{25}}{q_o U_o V^{0.66}}$	Fan air power coefficient
$CHT_5 = \frac{H_5 - P_o}{q_o}$	Jet total-head coefficient
$C_L = \frac{L}{q_o A}$	Wing lift coefficient
$CP_5 = \frac{P_5 - P_o}{q_o}$	Static base pressure coefficient @ Sta. 5
$CQ_5 = \frac{Q}{U_o V^{0.66}}$	Fan suction flow coefficient
$CT_w = \frac{T_w}{q_o V^{0.66}}$	Thrust coefficient for wing
$CT_o = \frac{T_o}{q_o V^{0.66}}$	Total thrust coefficient
d_5	Diameter of stern jet and of fan, ft
D	Diameter of fuselage, ft
F_w	Wing drag, lb
H_5	Jet total-head @ Sta. 5, lb/ft^2
ΔH_{25}	Total-head rise of fan between Sta. 2 and 5, lb/ft^2
L	Wing lift, lb
n	Fan speed, RPM
p_o	Free-stream static pressure, lb/ft^2
p_5	Static base pressure @ Sta. 5, lb/ft^2
$q_o = \frac{1}{2}\rho U_o^2$	Free-stream dynamic pressure, lb/ft^2
Q	Fan suction flow, ft^3/sec
T	Thrust of fuselage/boundary-layer control/jet system, lb
$u_t = \pi d_5 n$	Fan tip speed, ft/sec
U_o	Free-stream velocity, ft/sec
U_5	Jet velocity @ Sta. 5, ft/sec
V	Fuselage volume, ft^3
W_o	Gross weight, lb
$\varepsilon = \frac{W_o U_o}{HP550}$	Aerodynamic efficiency index
η_F	*Fan total efficiency*
ν	Kinematic viscosity of air, ft^2/sec
ρ	Mass density of air, $lb\ sec^2/ft^4$
$\phi = \frac{Q}{\frac{\pi}{4} d_5^2 u_t}$	Fan flow parameter
$\psi = \frac{\Delta H_{25}}{\frac{1}{2}\rho u_t^2}$	Fan pressure parameter

Introduction

The concept of the optimum aerodynamic integration of body pressure-distribution (with concomitant shape), slot-suction boundary-layer control and stern jet-propulsion was presented in 1967[1]; a wind-tunnel verification with a self-propelled test model was presented in 1982,[2] showing 50% power reduction as compared to the best streamlined body with stern wake-propeller. An optimized LTA system was derived from the above data[3] and it was also shown that jet-propulsion of a subsonic body with free transition was achieved with jet total-head equal to free-stream's.[4] It can be noted that, for the same mass flow, a conventional free-stream jet propulsor would have a jet total-head coefficient $CHT_5 = 4$ or, for the same diameter, a coefficient $CHT_5 = 2$, as shown in Ref. 5, on the basis of the best conventional streamlined body of equal volume.

The optimization of streamlined bodies by shape only was presented in 1974;[6] for all-turbulent boundary-layers, little drag gain could be obtained by optimizing the shape. This extensive program

*Consulting Engineer; Associate Fellow AIAA.

proved conclusively that boundary-layer control and propulsion had to be integrated with the body shape if substantial power gain had to be achieved.

The objective of this paper is to investigate heavier-than-air applications of this optimized system, i.e. to investigate the installation of a lifting wing onto the fuselage/boundary-layer control/jet propulsion system. The evaluation will be carried out on the basis of an aerodynamic efficiency index $\varepsilon = W_0 U_0/HP$ for two classes of aircraft, i.e. mini-RPV @ 100 and 150 Kn and small GA (General Aviation) 2-seat and 4-seat aircraft @ 200 MPH.

Optimized Body/Boundary-Layer Control/ Jet-Propulsion System: Wind-Tunnel Test

The wind-tunnel test program of the 20" diameter self-propelled model was carried out in 1981 in the 8x10 low-speed wind tunnel of the David Taylor Naval Ship R&D Center; the test program was quite extensive as it comprised over 800 test points organized in 86 test runs. The test results are presented in Refs. 2, 3 and 4. The basic test model with open jet (Conf. 00) is shown in Fig. 1 (starboard photo) and in Fig. 2 (stern photo). In Fig. 1 the 12" chord strut can be plainly seen as large as a wing would be; its interference effect is already accounted for in all the test results. Figure 2 shows clearly the three radial rakes in the jet nozzle to measure the flow and the jet total-head.

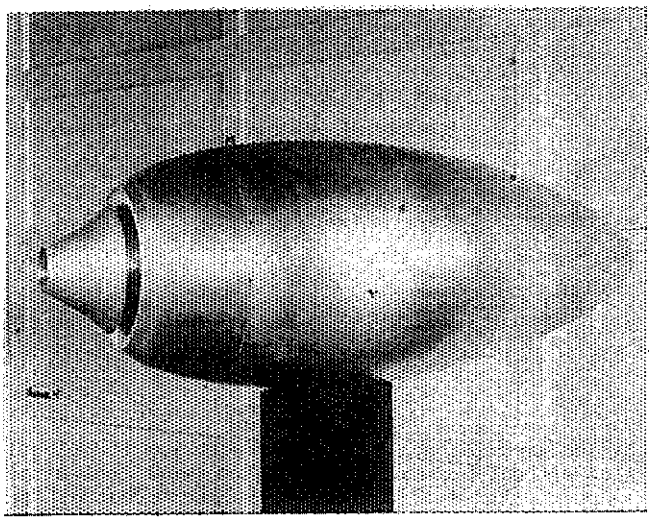

Fig. 1 Starboard photo of wind-tunnel test model (Conf. 00)

The axial force (drag or thrust) measurements were based both on the wake's momentum balance, as indicated by a wake rake, and on the force exerted on the strut, as indicated by the wind-tunnel balance which was supporting the strut.

At the higher thrust coefficients, above CT = 0.010, there was in all cases excellent agreement between the two types of axial force measurements, as shown in Figs. 7, 8 and 9; therefore the thrust data cannot be disputed in any way.

The model was also tested with a tailboom in the jet nozzle (Conf. 01) as shown in Fig. 3.

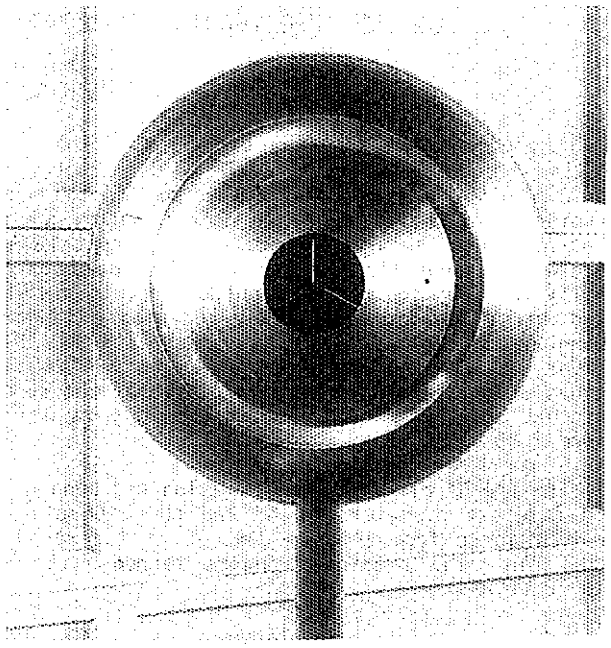

Fig. 2 Stern photo of wind-tunnel test model (Conf. 00)

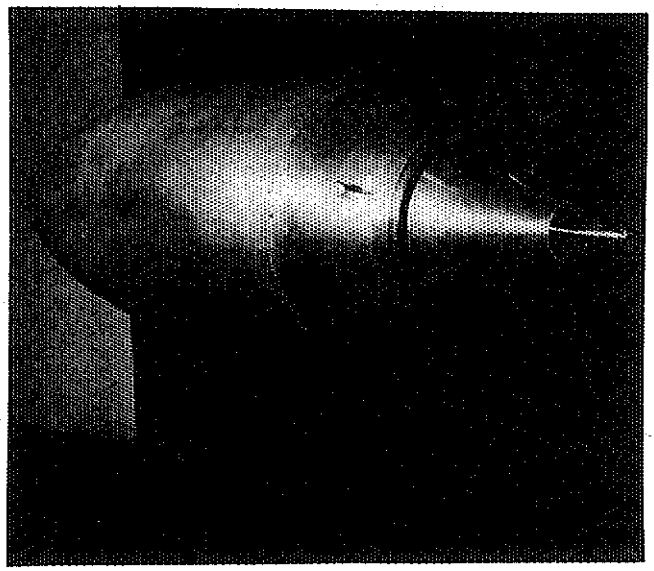

Fig. 3 Port photo of wind-tunnel test model with tailboom (Conf. 01)

The layout of the test model's aftbody with the suction slot, fan installation and jet nozzle is shown in Fig. 4. While the fan should have been at Station 5, the arrangement shown had to be accepted for practical reasons. The fan mass-flow weighted mean pressure rise is computed between Stations 2 and 5, with the flow being measured at Station 5; the fan air power is determined by the product of flow and pressure rise.

Figure 5 presents a photo of the axial fan installation in the forebody of the wind-tunnel test model; the fan discharge is in the left foreground, while the fan intake is indicated by the rounded edge inside the forebody.

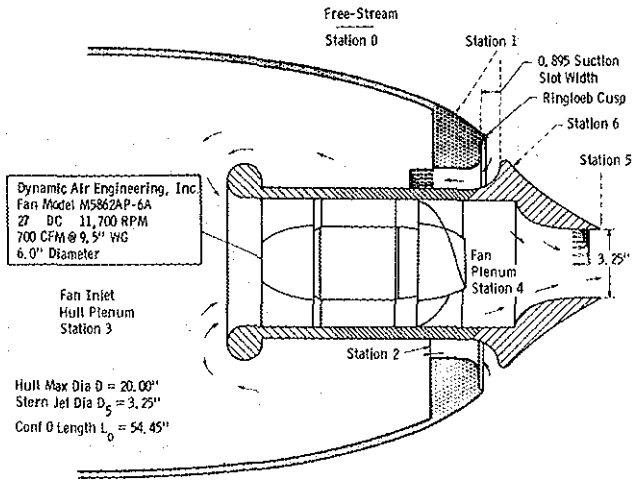

Fig. 4 Aftbody layout with suction-slot, fan installation and jet nozzle (Conf. 00)

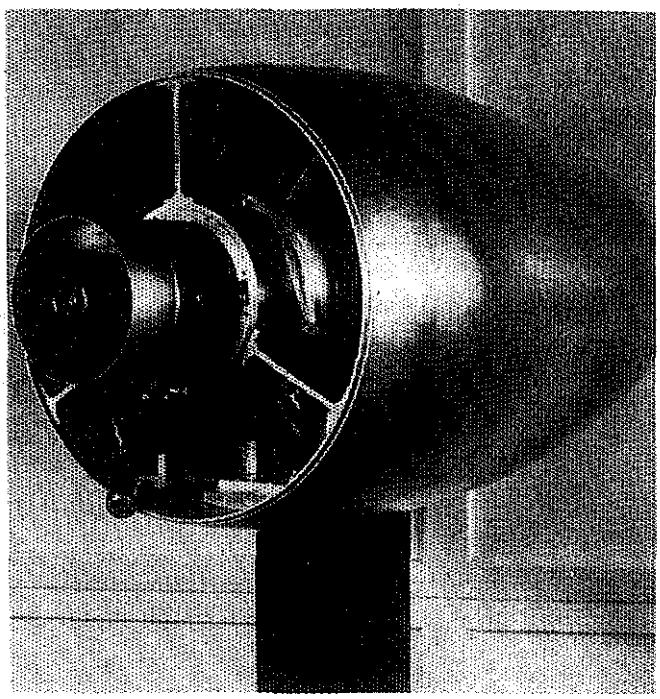

Fig. 5 Photo of fan installation in wind-tunnel test model

The typical stepwise static pressure distribution on the body is shown in Fig. 6 at 0° and 6° angle of attack. The stepwise distribution is used (with suitable boundary-layer control) to avoid the large growth of the boundary-layer momentum-thickness which normally occurs in the adverse pressure gradient area and to achieve very low external wake drags, as shown in Refs. 1 and 2.

While in Refs. 2, 3 and 4 the wind-tunnel test data were plotted only up to CT = 0.020, since the main focus was on the equilibrium point (CT = 0), in this paper all the available test data are plotted, for both free transition on the body and for transition tripped at 10% length.

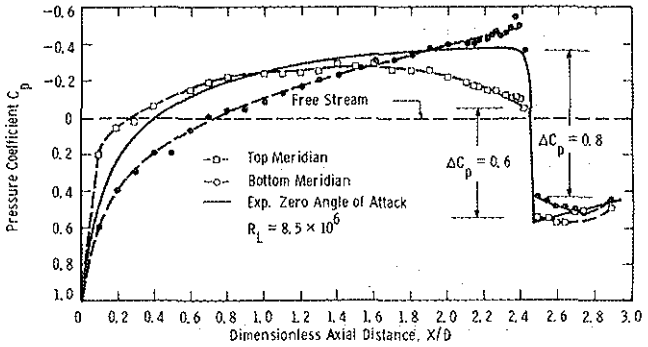

Fig. 6 Experimental static-pressure distribution on test model @ 6° angle of attack

System Analysis

A procedure has been developed for the addition of wings to the body and for the computation of the additional thrust acquired from the jet to counteract the wing's drag. The wing's lift/drag ratios have been computed from classical NACA data;[7] better results could be obtained with modern airfoils such as the Liebeck, the NASA GA(W)-1 and -2, etc. The fan performance has been based on the tested NASA axial rotor/stator stage 51B; the stage's design and experimental performance is given in Ref. 8.

The experimental wind-tunnel test data of Ref. 2 have been replotted in the complete thrust range and are shown in Figs. 7, 8, 9, 11, 12 and 13. The fan selection plot is given in Fig. 10, with the 51B performance curves relating pressure, flow and efficiency.

The computational procedure comprising 15 steps is given below:

1. Select the max. cruise speed U_o and the corresponding dynamic pressure q_o; determine or estimate the gross weight W_o.

2. Select fuselage diameter to yield adequate cabin space and/or equipment volume.

3. Assume lift coefficient C_L of wing @ max. cruising speed. Compute the wing loading $q_o C_L$ and the wing area $A = W_o/q_o C_L$. A lift coefficient $C_L = 0.40$ is selected for the mini-RPV and $C_L = 0.30$ is selected for the GA aircraft.

4. Compute the wing chord and span, assuming a wing aspect-ratio AR = 10 and constant chord:

$$C = \sqrt{\frac{A}{10}} \qquad B = 10C$$

Actually the wing may have a taper ratio and the computed chord value is the mean chord.

5. Compute the wing lift/drag ratio at the selected C_L point, using one of the following two experimental equations from Ref. 7 (Fig. 18, p. 21) for wings of aspect ratio AR = 10:

a. $C_D = 0.0068 + 0.0343\ C_L^2$ (NACA 23018 Airfoil)

b. $C_D = 0.0045 + 0.0383\ C_L^2$ (NACA 653-418 Airfoil)

A parametric wing design study should be made, in the manner of Koegler,[9] but it is beyond the scope of this brief paper.

6. Compute the drag of the wing:

$$F_W = \frac{W_o}{C_L/C_D}$$

since the wing lift must equal the gross weight W_o. Compute the thrust coefficient:

$$CT_W = \frac{F_W}{q_o V^{0.66}}$$

required to generate the thrust to counterbalance the wing drag. Add 10% to the wing thrust coefficient for wing/fuselage interference drag, although the model was tested in the wind-tunnel with a strut large enough to be a wing; also add another thrust coefficient increment of 0.003 for the empennage and tailbooms.

$$CT_o = CT_W + 0.10\ CT_W + 0.003$$

In the wind-tunnel tests of Ref. 2, an empennage adequate to yield neutral static stability to the body up to 8° had an incremental power coefficient of only 0.0020.

7. Obtain the value of the fan air power coefficient:

$$CHP_{25} = \frac{Q\Delta H_{25}}{q_o U_o V^{0.66}}$$

from the experimental plot CHP_{25} vs CT as presented in Fig. 7, corresponding to the above CT_o, for the free transition or for the tripped transition case, as warranted by the Reynolds number and by operational considerations.

8. Obtain the value of the fan flow coefficient:

$$CQ_5 = \frac{Q}{U_o V^{0.66}}$$

from the experimental plot CQ_5 vs CT as presented in Fig. 8, corresponding to the above CT_o, for the free transition or for the tripped transition case, as warranted by the Reynolds number and by operational considerations. Compute the fan flow $Q = CQ_5 \times U_o V^{0.66}$.

9. Obtain the value of the fan pressure-rise coefficient:

$$CH_{25} = \frac{\Delta H_{25}}{q_o}$$

from the experimental plot CH_{25} vs CT as presented in Fig. 9, corresponding to the above CT_o for the free transition or for the tripped transition case, as warranted by the Reynolds number and by operational considerations. Compute the fan pressure rise $\Delta H_{25} = CH_{25} \times q_o$.

10. The selection of the best axial rotor/stator stage for the job requires the computation of the fan system resistance coefficient ϕ^2/ψ in the ϕ/ψ domain:

$$\phi^2/\psi = \frac{CQ_5^2}{CH_{25}}\ 3557$$

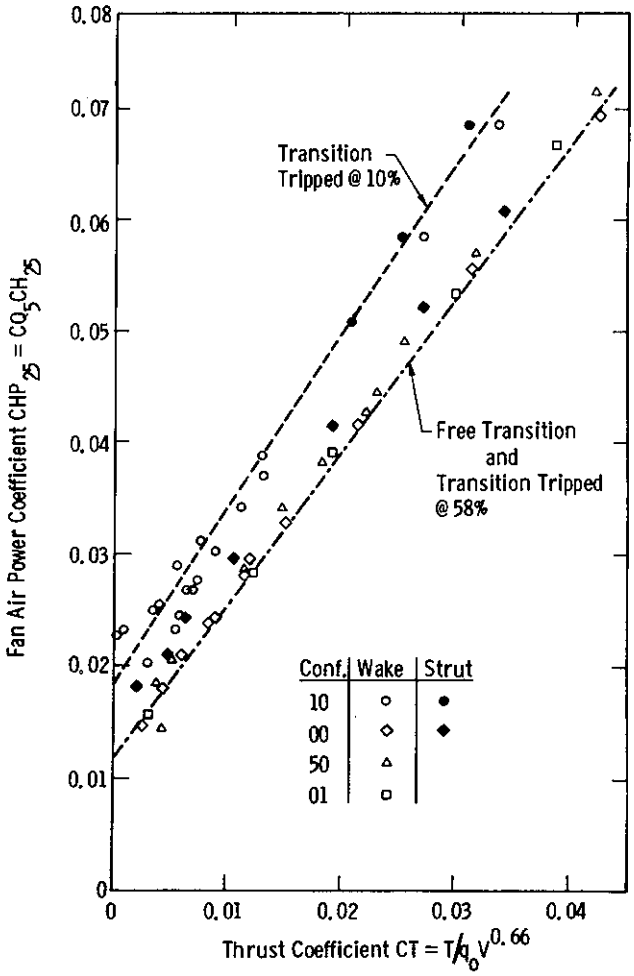

Fig. 7 Fan air power coefficient CHP_{25} vs Thrust coefficient CT

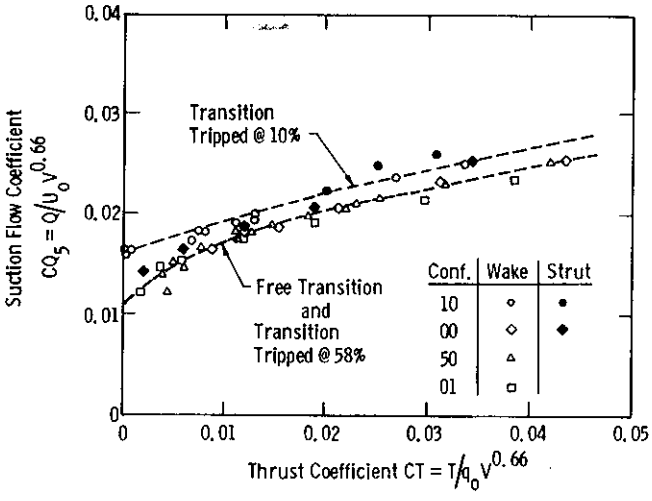

Fig. 8 Fan flow coefficient CQ_5 vs Thrust coefficient CT

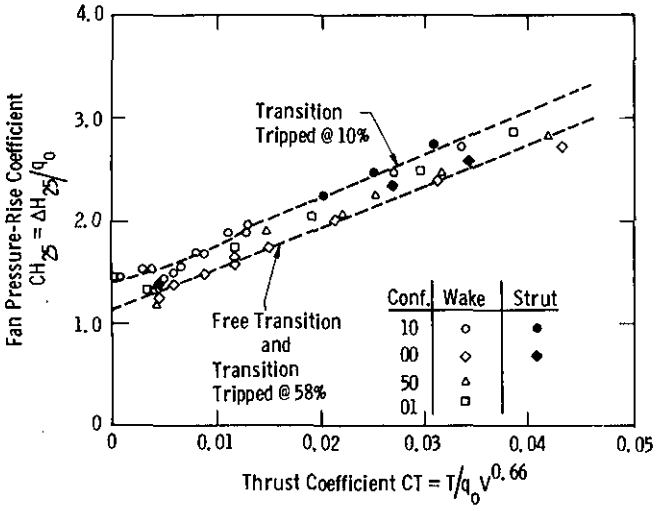

Fig. 9 Fan pressure-rise coefficient CH_{2S} vs Thrust coefficient CT

The denomination of ϕ is the fan flow parameter:

$$\phi = \frac{Q}{\frac{\pi}{4} d_5^2 u_t}$$

The denomination of ψ is the fan total-pressure parameter:

$$\psi = \frac{\Delta H_{2S}}{\frac{1}{2}\rho u_t^2}$$

The fan diameter corresponds to the jet diameter d_5; $u_t = \pi d_5 n$ is the fan tip speed and ρ is the air mass density. Figure 10 presents the ϕ-ψ plot with two fan system resistance curves, representing the max. and min. encountered in this study, and with the experimental performance curves ϕ-ψ and ϕ-η_F [8] of the selected NASA axial rotor/stator stage 51B; it can be seen that a fairly good match is achieved, i.e. the fan will operate between 88.3 and 90.6% efficiency. Fan aerodynamic selection procedures are discussed thoroughly in Section 6 of Ref. 10.

11. The fan speed is computed:

$$n = \frac{CQ_5}{\phi} \frac{U_0}{V^{0.33}} 130.13 \text{ RPS}$$

The value of the fan flow parameter ϕ is determined in Fig. 10 from the intersection of the fan system resistance curve with the NASA 51B performance curve. The range of ϕ is from 0.485 to 0.508. Similarly, the fan efficiency η_F is determined in Fig. 10 from the NASA 51B efficiency curve at the above ϕ location.

The fan diameter is assumed to correspond to the stern jet diameter: $d_5 = 0.1625\,D$.

12. The fan shaft power can be computed now from the CHP_{2S} value of Step 7 and the above efficiency determination for an available fan design:

$$HP = \frac{CHP_{2S} q_0 U_0 V^{0.66}}{\eta_F \; 550}$$

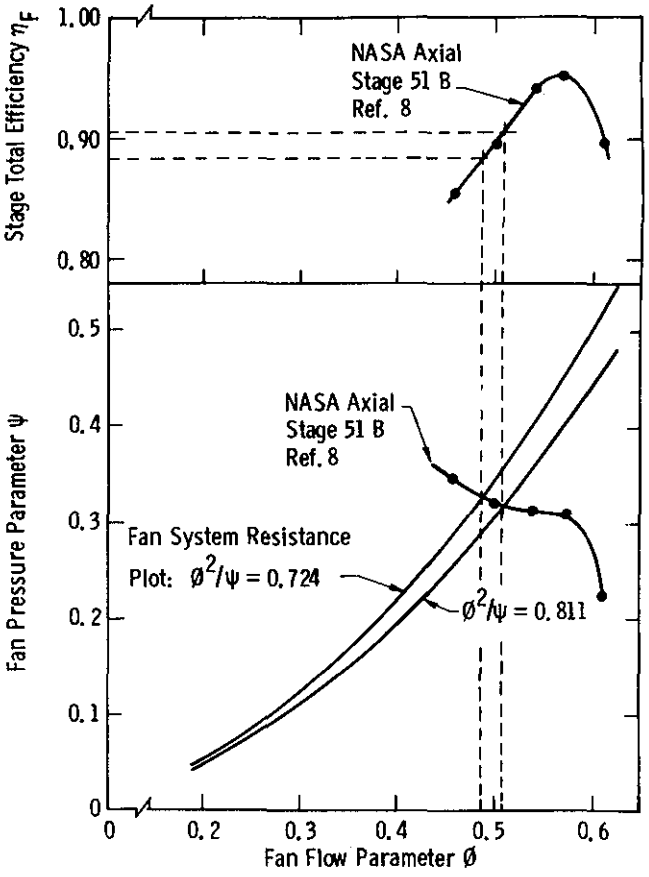

Fig. 10 Fan pressure parameter ψ and total efficiency η_F vs fan flow parameter ϕ

13. The jet total-head coefficient

$$CHT_5 = \frac{H_5 - p_0}{q_0}$$

is determined from the plot of Fig. 11 and the jet velocity ratio U_5/U_0 is determined from the plot of Fig. 12 for the free transition or the tripped transition cases, as warranted by Reynolds number and operational considerations.

14. The jet static base pressure coefficient CP_5 is determined from the plot of Fig. 13. It can be seen that the static base pressure coefficient range is very high; CP_5 will be over 0.8 for the thrust coefficient range of this study. As a reference, Ref. 11 shows that the base pressure coefficient of conventional boattail/jet afterbodies is in the 0.10 to 0.15 range.

15. The final step is the computation of the aerodynamic efficiency index:

$$\varepsilon = \frac{W_0 U_0}{HP550}$$

The index expresses the power required to fly the aircraft's gross weight at the max. cruise speed; therefore, it is a good indication of the efficiency of the aerodynamic design when comparing two aircraft at the same speed.

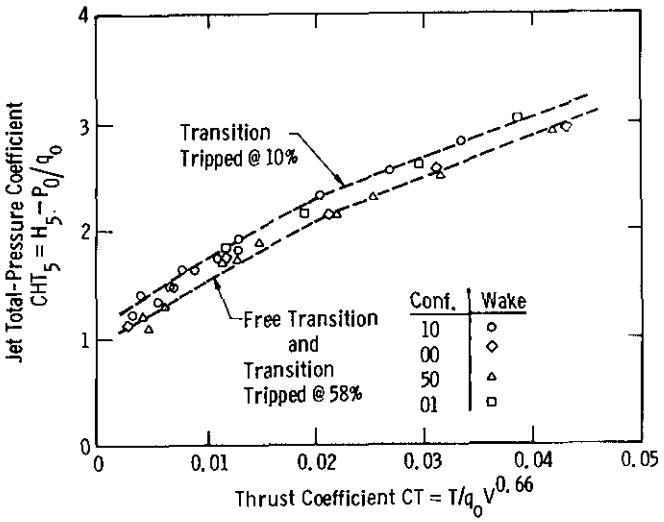

Fig. 11 Jet total-head coefficient CHT_5 vs Thrust coefficient CT

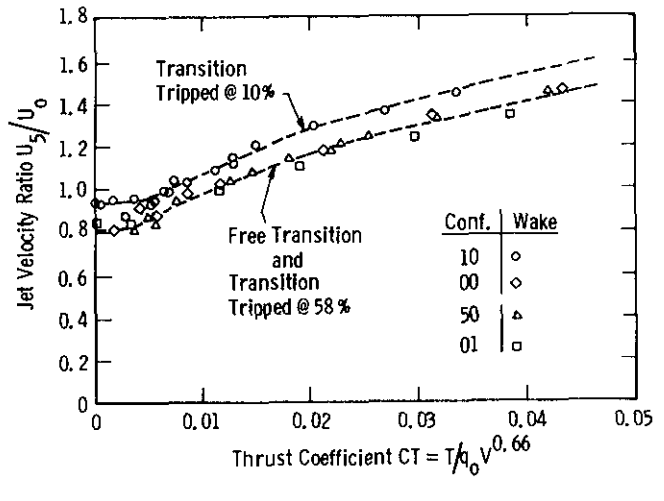

Fig. 12 Jet velocity-ratio U_5/U_0 vs Thrust coefficient CT

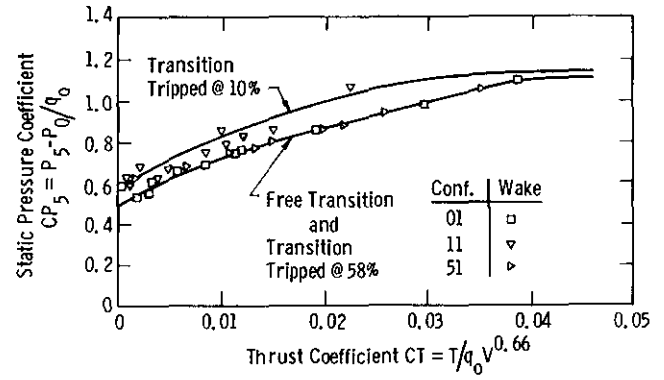

Fig. 13 Jet static base pressure coefficient CP_5 vs Thrust coefficient CT

Mini-RPV

Mini-RPV aerodynamic design has not achieved yet an adequate degree of efficiency for the mission speed and endurance requirements. Considering typical current vehicles such as the Air Force/Boeing Pave Tiger, the Army/Lockheed Aquila, the Israel Aircraft Industries Scout, the Tadiran Mastiff MK3 and the Developmental Sciences Sky Eye, it is found that the gross weight ranges from 220 to 380 lb, the maximum cruising speed ranges from 85 to 100 Kn and the engine powers range from 22 to 30 HP. The aerodynamic efficiency index ranges from 2.5 to 3.5.

The wind-tunnel test model,[2,3,4] with its diameter D = 20.0 in. and 100 Kn speed, may be classified as a full-scale mini-RPV; Table 1 presents its performance data for 125, 150 and 175 lb gross weights with a suitable wing (C_L = 0.40) and empennage.

Table 1 20" Diameter (V = 6.2 ft³) Mini-RPV @ 100 Kn (q_0 = 34.1 PSF)
(Free Transition)

Gross Weight W_0 lb	125 lb	150 lb	175 lb
Wing loading $q_0 C_L$ @ C_L= 0.4 PSF	13.6	13.6	13.6
Wing area $A = W_0/q_0 C_L$, ft^2	9.19	11.03	12.86
Wing chord, C ft	0.958	1.050	1.134
Wing span, B ft	9.58	10.50	11.34
Lift/drag ratio of wing, C_L/C_D @ C_L = 0.40	37.6	37.6	37.6
Drag of wing, $F_W = W_0/\frac{C_L}{C_D}$	3.32	3.99	4.65
Thrust coeff. for wing CT_W	0.0289	0.0348	0.0406
Total thrust coeff. CT_0	0.0348	0.0412	0.0476
Fan air power coeff. CHP_{2s}	0.060	0.0685	0.0755
Fan flow coeff. CQ_5	0.0237	0.0252	0.0264
Fan flow Q CFS	13.50	14.35	15.03
Fan pressure-rise coeff. CH_{2s}	2.54	2.80	3.05
Fan pressure-rise ΔH_{2s} PSF	86.36	95.20	103.70
Fan system-resistance coeff. ϕ^2/ψ	0.785	0.805	0.811
Fan speed, n RPM	33,964	35,756	37,311
Fan diameter, d_5 in.	3.25	3.25	3.25
Fan efficiency, η_F %	89.75	90.50	90.75
Fan shaft power HP	2.35	2.78	3.12
Jet total-head coeff. CHT_5	2.66	2.90	3.16
Jet velocity ratio U_5/U_0	1.35	1.42	1.51
Jet static base pressure coeff. CP_5	1.04	1.10	1.10
Aerodynamic efficiency index ε	16.34	17.20	18.22

With free transition the fan shaft powers are 3 HP and less at the 100 Kn speed; the aerodynamic efficiency index is over 16. The engine may be an available Fox Twin, yielding 3 HP @ 14,500 RPM and weighing 3 lb with mount and muffler. Table 2 presents the performance data of the same 20 in. fuselage at 150 Kn speed with free transition, while Table 2a presents the corresponding data with transition tripped @ 10% length on the fuselage, for gross weights of 150, 175 and 200 lb. It is found that the fan shaft powers are less than 7 HP with free transition and less than 8 HP with tripped transition; the corresponding aerodynamic efficiency index values are over 13 and 10, respectively.

As a direct comparison with a current mini-RPV design, the fuselage diameter was increased to 34 in. to match both the lateral dimension and the length of the Air Force/Boeing Pave Tiger's fuselage; Table 3 presents the performance data @ 100 Kn with free transition while Table 3a presents the corresponding data with transition tripped @ 10% length, for gross weights of 225, 250 and 275 lb.

Table 2 20" Diameter (V = 6.2 ft³) Mini-RPV @ 150 Kn (q_o = 77.3 PSF)
(Free Transition)

Gross Weight W_o lb	150 lb	175 lb	200 lb
Wing loading q_oC_L @ C_L=0.4 PSF	30.8	30.8	30.8
Wing area $A = W_o/q_oC_L$, ft²	4.87	5.68	6.49
Wing chord, C ft	0.697	0.753	0.805
Wing span, B	6.97	7.53	8.05
Lift/drag ratio of w' C_L/C_D @ C_L = 0.40	37.6	37.6	37.6
Drag of wing, $F_W = W_o/\frac{C_L}{C_D}$	3.99	4.65	5.32
Thrust coeff. for wing CT_W	0.0153	0.0179	0.0205
Total thrust coeff. CT_o	0.0198	0.0226	0.0255
Fan air power coeff. CHP_{25}	0.0395	0.0432	0.0471
Fan flow coeff. CQ_5	0.0202	0.0210	0.0216
Fan flow Q CFS	17.20	17.89	18.40
Fan pressure-rise coeff. CH_{25}	1.94	2.05	2.16
Fan pressure-rise ΔH_{25} PSF	150.0	158.8	166.9
Fan system-resistance coeff. ϕ^2/ψ	0.746	0.763	0.766
Fan speed, n RPM	44,071	45,412	46,617
Fan diameter, d_5 in.	3.25	3.25	3.25
Fan efficiency, η_F %	89.0	89.6	89.7
Fan shaft power HP	5.29	5.74	6.26
Jet total-head coeff. CHT_5	2.06	2.20	2.30
Jet velocity ratio U_5/U_o	1.16	1.20	1.25
Jet static base pressure coeff. CP_5	0.86	0.89	0.93
Aerodynamic efficiency index ε	13.00	14.00	14.69

With free transition the fan shaft powers are less than 6 HP while with tripped transition the powers are less than 20 HP; this may be compared with the 28 HP engine of the 250 lb Pave Tiger. The aerodynamic efficiency index values are over 14 and 11, respectively.

Finally, Table 4 presents the performance data of the 34 in. diameter fuselage at 150 Kn with gross weights of 250, 275 and 300 lb and with tripped transition. It can be noted that this case with 300 lb represents a substantial performance improvement over the Pave Tiger, in both speed (50% gain) and weight (20% gain); the fan shaft power is 16 HP and the aerodynamic efficiency index is 8.75. It can be noted that, with tripped transition, there is no laminar flow risk and that the turbulent power coefficients should actually be lower because the Reynolds number is higher by the factor 1.7 x 1.5 = 2.55.

A schematic layout of the proposed mini-RPV configuration is shown in Fig. 14; the pylon/wing arrangement was proposed by Larrabee[12] for gliders so as to maximize the wing's lift. It can be noted that the pylon/fuselage interference effect was already simulated in the wind-tunnel tests by the strut. The wing span is 162 in. and the useful fuselage length is 83 in., while the overall fuselage length is 127 in. The empennage is supported by a single boom.

Small General Aviation Aircraft

Small GA aircraft comprise another category, to which this system analysis may be applied with interesting results.

Table 2a 20" Diameter (V = 6.2 ft³) Mini-RPV @ 150 Kn (q_o = 77.3 PSF)
(Transition Tripped @ 10% Length)

Gross Weight W_o lb	150 lb	175 lb	200 lb
Total thrust coeff. CT_o	0.0198	0.0226	0.0255
Fan air power coeff. CHP_{25}	0.050	0.0543	0.0587
Fan flow coeff. CQ_5	0.0222	0.0227	0.0234
Fan flow Q CFS	18.9	19.3	19.9
Fan pressure-rise coeff. CH_{25}	2.24	2.35	2.48
Fan pressure-rise ΔH_{25} PSF	173.1	181.6	191.7
Fan system-resistance coeff. ϕ^2/ψ	0.781	0.778	0.783
Fan speed, n RPM	49,034	49,835	50,140
Fan diameter, d_5 in.	3.25	3.25	3.25
Fan efficiency, η_F %	88.3	89.9	90.2
Fan shaft power HP	6.75	7.19	7.75
Jet total-head coeff. CHT_5	2.28	2.40	2.50
Jet velocity ratio U_5/U_o	1.28	1.32	1.36
Jet static base pressure coeff. CP_5	0.98	1.02	1.06
Aerodynamic efficiency index ε	10.40	11.19	11.84

Table 3 34" Diameter (V = 30.5 ft³) Mini-RPV @ 100 Kn (q_o = 34.1 PSF)
(Free Transition)

Gross Weight W_o lb	225 lb	250 lb	275 lb
Wing loading q_oC_L @ C_L=0.4 PSF	13.6	13.6	13.6
Wing area A = W_o/q_oC_L, ft²	16.5	18.4	20.2
Wing chord, C ft	1.284	1.356	1.421
Wing span, B ft	12.84	13.56	14.21
Lift/drag ratio of wing, C_L/C_D @ C_L = 0.40	37.6	37.6	37.6
Drag of wing, $F_W = W_o/\frac{C_L}{C_D}$	5.98	6.65	7.31
Thrust coeff. for wing CT_W	0.0180	0.0201	0.0221
Total thrust coeff. CT_o	0.0228	0.0251	0.0273
Fan air power coeff. CHP_{25}	0.0436	0.0466	0.0495
Fan flow coeff. CQ_5	0.0210	0.0216	0.0220
Fan flow Q CFS	34.95	35.94	36.60
Fan pressure-rise coeff. CH_{25}	2.05	2.14	2.23
Fan pressure-rise ΔH_{25} PSF	69.9	72.9	76.0
Fan system-resistance coeff. ϕ^2/ψ	0.763	0.773	0.770
Fan speed, n RPM	17,916	18,354	18.619
Fan diameter, d in.	5.525	5.525	5.525
Fan efficiency, η_F %	89.10	89.40	89.60
Fan shaft power HP	4.98	5.29	5.65
Jet total-head coeff. CHT_5	2.20	2.30	2.38
Jet velocity ratio U_5/U_o	1.20	1.24	1.26
Jet static base pressure coeff. CP_5	0.90	0.92	0.95
Aerodynamic efficiency index ε	14.0	14.6	15.1

Table 4 34" Diameter (V = 30.5 ft³) Mini-RPV @ 150 Kn (q_o = 77.3 PSF)
(Transition Tripped @ 10% Length)

Gross Weight W_o lb	250 lb	275 lb	300 lb
Wing loading q_oC_L @ C_L=0.4 PSF	30.8	30.8	30.8
Wing area A = W_o/q_oC_L, ft²	8.11	8.93	9.74
Wing chord, C ft	0.900	0.945	0.986
Wing span, B ft	9.00	9.45	9.86
Lift/drag ratio of wing, C_L/C_D @ C_L = 0.40	37.6	37.6	37.6
Drag of wing, $F_W = W_o/\frac{C_L}{C_D}$ lb	6.65	7.31	7.98
Thrust coeff. for wing CT_W	0.0089	0.0098	0.0106
Total thrust coeff. CT_o	0.0128	0.0138	0.0146
Fan air power coeff. CHP_{25}	0.0390	0.0405	0.0416
Fan flow coeff. CQ_5	0.0198	0.0202	0.0205
Fan flow Q CFS	48.8	49.8	50.5
Fan pressure-rise coeff. CH_{25}	1.92	1.98	2.02
Fan pressure-rise ΔH_{25} PSF	148.4	153.0	156.3
Fan system-resistance coeff. ϕ^2/ψ	0.724	0.731	0.738
Fan speed, n RPM	25,862	26,276	26,557
Fan diameter, d in.	5.525	5.525	5.525
Fan efficiency, η_F %	88.4	88.6	88.8
Fan shaft power HP	15.00	15.70	16.20
Jet total-head coeff. CHT_5	1.90	1.96	2.00
Jet velocity ratio U_5/U_o	1.15	1.16	1.18
Jet static base pressure coeff. CP_5	0.87	0.89	0.90
Aerodynamic efficiency index ε	7.72	8.19	8.75

Table 3a 34" Diameter (V = 30.5 ft³) Mini-RPV @ 100 Kn (q_o = 34.1 PSF)
(Transition Tripped @ 10% Length)

Gross Weight W_o lb	225 lb	250 lb	275 lb
Total thrust coeff. CT_o	0.0228	0.0251	0.0273
Fan air power coeff. CHP_{25}	0.0546	0.0580	0.0612
Fan flow coeff. CQ_5	0.0228	0.0233	0.0237
Fan flow Q CFS	37.94	38.76	39.43
Fan pressure-rise coeff. CH_{25}	2.36	2.45	2.54
Fan pressure-rise ΔH_{25} PSF	80.47	83.54	86.6
Fan system-resistance coeff. ϕ^2/ψ	0.781	0.786	0.785
Fan speed, n RPM	19,296	19,680	20,018
Fan diameter, d_5 in.	5.525	5.525	5.525
Fan efficiency, η_F %	89.5	89.8	89.8
Fan shaft power HP	6.19	6.55	6.90
Jet total-head coeff. CHT_5	2.40	2.48	2.56
Jet velocity ratio U_5/U_o	1.33	1.36	1.38
Jet static base pressure coeff. CP_5	1.03	1.06	1.08
Aerodynamic efficiency index ε	11.22	11.74	12.26

Table 5 lists the pertinent parameters of three current 2-seat personal GA aircraft by Beech, Cessna and Piper; the gross weight is nearly the same (1670 to 1675 lb) and so is the speed (121 to 127 MPH) and the engine power (108 to 115 HP). The aerodynamic efficiency index is in the vicinity of 5.0.

The fuselage diameter is selected at 45 in. so as to accommodate two tandem seats; the cabin arrangement layout is shown in Fig. 15. It has been observed that minimum cabin height is 42 in. and the minimum seat spacing dimension is 36 in.

The speed has been selected to be 200 MPH instead of 125 MPH because it represents present GA speed for small personal aircraft. Table 6 presents the performance data for gross weights of 1400, 1675 and 1800 lb with tripped transition. It can be seen that the fan shaft power is less than 72 HP and the aerodynamic efficiency index is over 12.0. This performance yields a 60% speed improvement, a 33% power gain and a 7.5% gross weight enhancement. The schematic layout of this 2-seat GA configuration is shown in Fig. 16, with a mid-wing arrangement with 0.45 taper ratio and 277 in. overall span. The useful fuselage length is 110 in. while the overall fuselage length is 130 in. The empennage is supported by a twin boom and it comprises twin rudders.

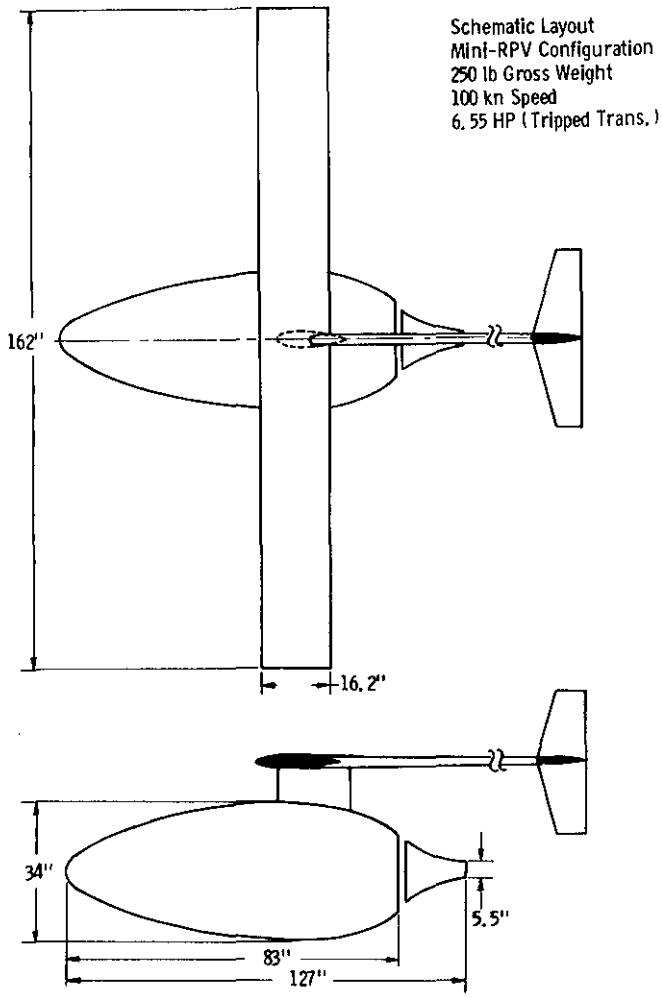

Fig. 14 Schematic layout of mini-RPV configuration

Table 5 2-Seat GA Aircraft @ 120 MPH (q_o = 37.0 PSF)

			Beech 77 Skipper	Cessna 152 Aerobat	Piper PA-38-112 Tomahawk 2
Empty weight	W	lb	1,103	1,133	1,128
Gross weight	W_o	lb	1,675	1,675	1,670
Wing span	B	ft	30.0	33.3	34.0
Wing area	A	ft^2	130	160	124.7
Wing loading	W/A	PSF	12.88	10.46	13.39
Length	ℓ	ft	24.0	24.1	23.1
Engine power		HP	115	108	112
Max. cruise speed	U_o	MPH	121	122	127
Wing lift coeff.	C_L		0.341	0.272	0.322
Aerodynamic efficiency index		ε	4.70	5.04	5.05

Note: The above data were derived from Aviation Week & Space Technology, March 12, 1984, p. 144.

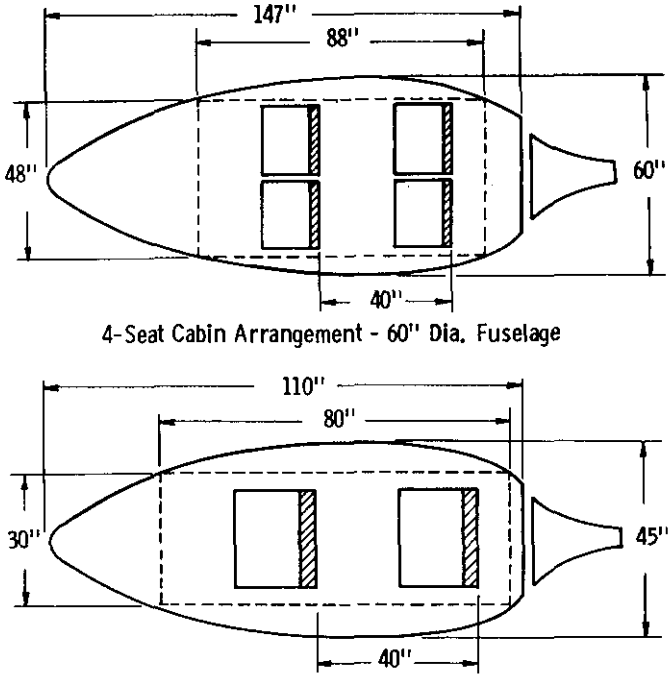

Fig. 15 Cabin arrangement layout for GA aircraft

Table 6 45" Diameter (V = 70.6 ft^3) GA Aircraft @ 200 MPH (q_o = 104 PSF)
(Transition Tripped @ 10% Length)

Gross Weight W_o lb	1400 lb	1675 lb	1800 lb
Wing loading q_oC_L @ C_L=0.3 PSF	31.2	31.2	31.2
Wing area $A = W_o/q_oC_L$, ft^2	44.8	53.7	57.7
Mean wing chord, C ft	2.11	2.31	2.40
Wing span, B ft	21.1	23.1	24.0
Lift/drag ratio of wing, C_L/C_D @ C_L = 0.30	38.3	38.3	38.3
Drag of wing, $F_W = W_o/\frac{C_L}{C_D}$ lb	36.5	43.7	47.0
Thrust coeff. for wing CT_W	0.0206	0.0247	0.0265
Total thrust coeff. CT_o	0.0256	0.0301	0.0321
Fan air power coeff. CHP_{2s}	0.0588	0.0656	0.0685
Fan flow coeff. CQ_5	0.0234	0.0244	0.0248
Fan flow Q CFS	117.1	122.1	124.1
Fan pressure-rise coeff. CH_{2s}	2.45	2.66	2.74
Fan pressure-rise ΔH_{2s} PSF	254.8	276.6	284.9
Fan system-resistance coeff. ϕ^2/ψ	0.793	0.794	0.796
Fan speed, n RPM	25,777	26,825	27,211
Fan diameter, d_5 in.	7.31	7.31	7.31
Fan efficiency, η_F %	90.1	90.2	90.3
Fan shaft power HP	60.6	68.6	71.6
Jet total-head coeff. CHT_5	2.5	2.66	2.74
Jet velocity ratio U_5/U_o	1.37	1.41	1.44
Jet static base pressure coeff. CP_5	0.92	1.10	1.11
Aerodynamic efficiency index ε	12.1	13.0	13.3

Table 7 lists the pertinent parameters of five current 4-seat GA aircraft by Maule, Mooney, Piper, Cessna and Beech, with speed from 196 to 201 MPH, gross weights from 2500 to 3400 lb and engine powers from 200 to 285 HP. The aerodynamic efficiency index ranges from 6.5 to 7.9.

The cabin dimensions for four seats are typically 43 in. width, 48 in. height and 92 in. length; a fuselage diameter of 60 in. has been selected and the cabin layout arrangement is shown in Fig. 15.

Table 8 presents the performance data for gross weights of 2500, 2900 and 3400 lb at 200 MPH with tripped transition. It is seen that for the lowest weight the fan shaft power is 110, for a gain of 47%; for the middle weight the fan power is 120 HP, for a gain of 40%, while for the top weight the fan power is 132 HP, for a gain of 53%.

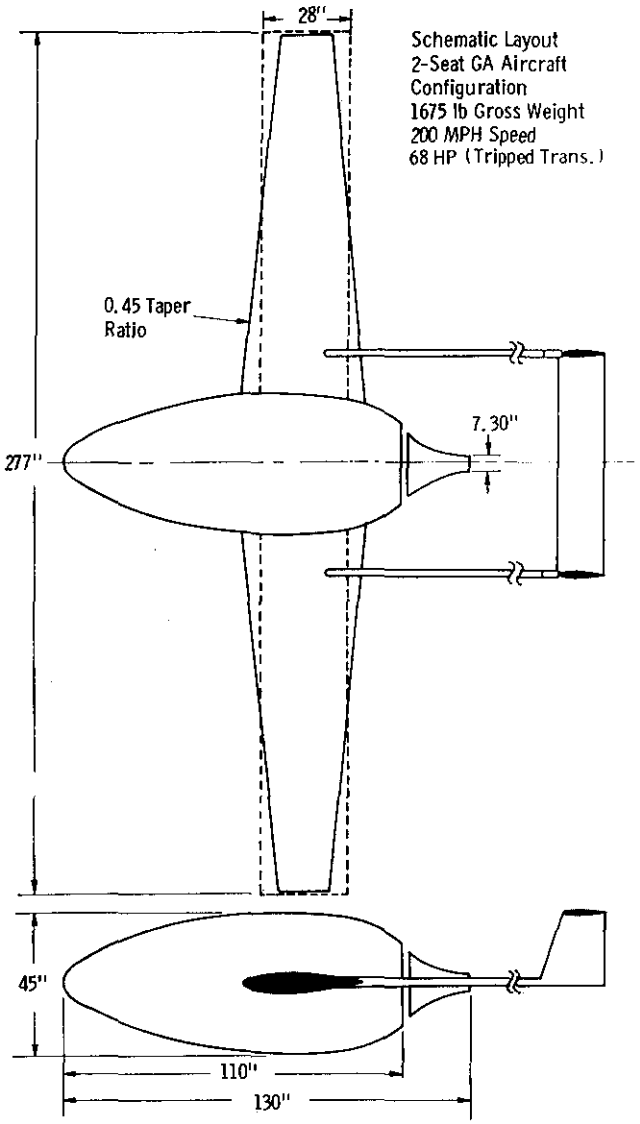

Fig. 16 Schematic layout of 2-seat GA aircraft configuration

Table 7 4-Seat GA Aircraft @ 200 MPH (q_o = 104 PSF)

			Maule M5-210 TC	Mooney M20J-201	Piper PA-28RT-201 Arrow 4	Cessna Turbo 182 Skylane RG	Beech F-33A Bonanza
Empty weight	W	lb	1400	1670	1692	1806	2125
Gross weight	W_o	lb	2500	2740	2900	3110	3400
Wing span	B	ft	30.9	36.1	35.4	36.0	33.5
Wing area	A	ft^2	157.9	175.0	170.0	174.0	181.0
Wing loading	$\frac{W_o}{A}$	PSF	15.8	15.6	17.05	17.8	18.8
Length	ℓ	ft	24.4	24.7	27.3	28.6	26.7
Engine power		HP	210.0	200.0	200.0	235.0	285.0
Max. cruise speed	U_o	MPH	196.0	201.0	198.0	199.0	198.0
Wing lift coeff.	C_L		0.157	0.148	0.167	0.172	0.184
Aerodynamic efficiency index		ε	6.49	7.47	7.90	7.22	6.50

Note: The above data were derived from Aviation Week & Space Technology, March 12, 1984, p. 144.

Table 8 60" Diameter (V = 167.4 ft^3) GA Aircraft @ 200 MPH (q_o = 104 PSF)
(Transition Tripped @ 10% Length)

Gross Weight	W_o	lb	2500 lb	2900 lb	3400 lb
Wing loading q_oC_L @ C_L=0.3		PSF	31.2	31.2	31.2
Wing area $A = W_o/q_oC_L$,		ft^2	80.1	92.9	108.9
Mean wing chord, C		ft	2.83	3.04	3.30
Wing span, B		ft	28.3	30.4	33.0
Lift/drag ratio of wing, C_L/C_D @ C_L = 0.30			38.3	38.3	38.3
Drag of wing, $F_W = W_o/\frac{C_L}{C_D}$		lb	65.2	75.7	88.7
Thrust coeff. for wing	CT_W		0.0207	0.0240	0.0281
Total thrust coeff.	CT_o		0.0257	0.0294	0.0339
Fan air power coeff.	CHP_{25}		0.0590	0.0644	0.0712
Fan flow coeff.	CQ_5		0.0235	0.0242	0.0252
Fan flow Q		CFS	209.4	215.6	224.5
Fan pressure-rise coeff.	CH_{25}		2.48	2.64	2.82
Fan pressure-rise ΔH_{25}		PSF	257.9	274.5	293.2
Fan system-resistance coeff.	ϕ^2/ψ		0.790	0.787	0.800
Fan speed, n		RPM	19,422	19,960	20,744
Fan diameter, d_5		in.	9.75	9.75	9.75
Fan efficiency, η_F		%	90.0	90.2	90.4
Fan shaft power		HP	110.3	120.1	132.5
Jet total-head coeff.	CHT_5		2.50	2.64	2.81
Jet velocity ratio	U_5/U_o		1.37	1.41	1.46
Jet static base pressure coeff.	CP_5		1.06	1.09	1.12
Aerodynamic efficiency index	ε		12.08	12.88	13.68

The aerodynamic efficiency index is over 12.0. The schematic layout of the 4-seat GA configuration is shown in Fig. 17; a high-wing arrangement was selected with a span of 360 in. and a 0.45 taper ratio. The useful fuselage length is 147 in. while the overall fuselage length is 174 in. The empennage is supported by twin booms and it comprises twin rudders.

Conclusions

It has been shown that the simple addition of a conventional NACA wing to the tested optimized system comprising axisymmetric body, boundary-layer control and stern jet propulsion yields a predicted aircraft performance which is superior to current mini-RPV and small GA aircraft levels.

A 250 lb gross weight mini-RPV could be flown at 100 Kn with 7.0 HP; a 2-seat 1675 lb GA aircraft could be flown at 200 MPH with 69 HP, and a 4-seat 2900 lb GA aircraft could be flown at 200 MPH with 120 HP.

The general trend of the aerodynamic efficiency index ε against the thrust coefficient CT is shown in Fig. 18 for both free transition and transition tripped at 10% length; it can be seen that the thrust coefficient should be kept above a value of 0.025 in order to achieve aerodynamic efficiency index values above 12.0. This can be done by adjusting the gross weight W_0 against the fuselage volume V and the speed U_0.

Better results can be expected if the lift system should be integrated, i.e. if the fuselage suction air mass flow should be directed laterally into the wings to supply jet flaps or circulation-control wall-jets. The limitation then would be the allowable wing loading and the wing's induced drag, as the lift coefficient is substantially increased by the jet-flap or by the circulation-control.

The air mass flow would serve three purposes: (a) fuselage boundary-layer control, (b) wing lift enhancement, and (c) propulsion. Also the suction's momentum drag is minimized since only the inner boundary-layer flow is drawn into the slot at Sta. 1 (Fig. 5); it is estimated that a 33% drag saving is achieved, as compared to free-stream flow intake, at the point of equilibrium for the body alone. The next step of this program is expected to be the wind-tunnel test of the 20 in. diameter model in the arrangement of Fig. 14; the wing pylon would be installed exactly as the present strut. A second step would be the investigation of the optimum fineness ratio; the 2.72 fineness ratio was selected originally for LTA application. A preliminary theoretical parametric study indicates that the optimum should be near 6 and that further power reduction can be expected.

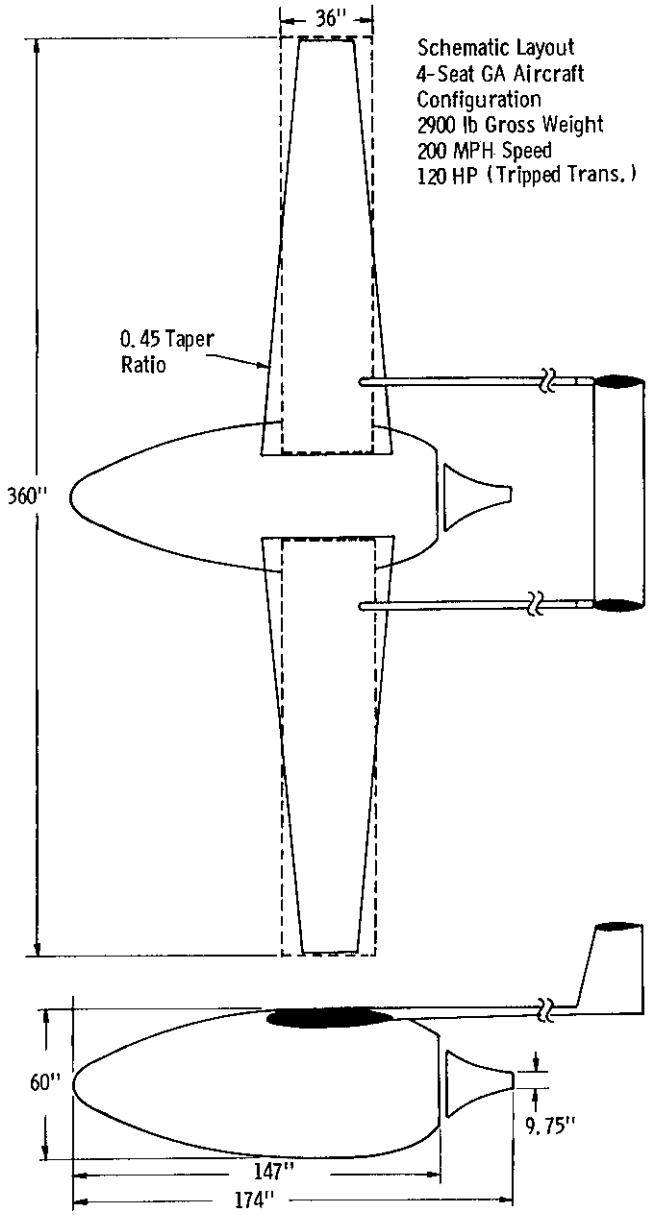

Fig. 17 Schematic layout of 4-seat GA aircraft configuration

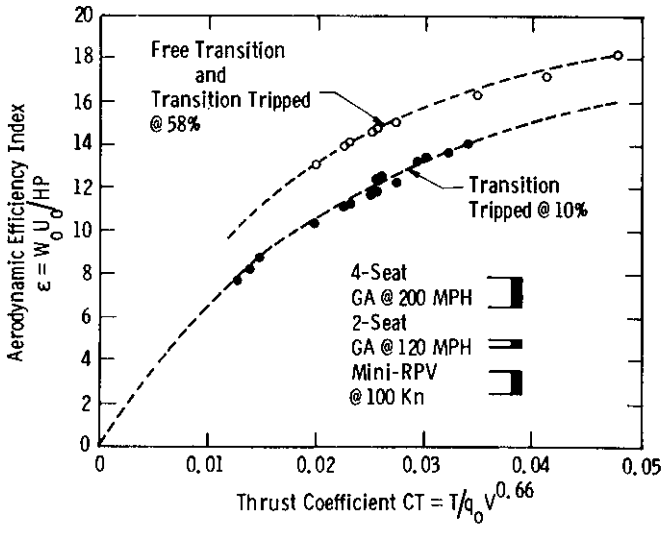

Fig. 18 Aerodynamic efficiency index ε vs Thrust coefficient CT

References

1. F. R. Goldschmied, "Integrated Hull Design, Boundary-Layer Control and Propulsion of Submerged Bodies," AIAA Journal of Hydronautics, Vol. 1, No. 1, pp. 1-11 (July 1967).

2. F. R. Goldschmied, "Integrated Hull Design, Boundary-Layer Control and Propulsion of Submerged Bodies: Wind-Tunnel Verification," AIAA Paper 82-1204, AIAA/SAE/ASME 18th Joint Propulsion Conference, Cleveland, OH (June 1982).

3. F. R. Goldschmied, "Wind-Tunnel Demonstration of an Optimized LTA System with 65% Power Reduction and Neutral Static Stability," AIAA Paper 83-1981, AIAA Lighter-Than-Air Systems Conference, Anaheim, CA (July 1983).

4. F. R. Goldschmied, "Jet-Propulsion of Subsonic Bodies with Jet Total-Head Equal to Free-Stream's," AIAA Paper 83-1790, AIAA Applied Aerodynamics Conference, Danvers, MA (July 1983).

5. F. R. Goldschmied, "Aerodynamic Integration of Axisymmetric Body Pressure-Distribution, Slot-Suction Boundary-Layer Control and Stern Jet-Propulsion, II - Propulsion Evaluation," AIAA Journal of Aircraft (to be published).

6. J. S. Parsons, R. E. Goodson and F. R. Goldschmied, "Shaping of Axisymmetric Bodies for Minimum Drag in Incompressible Flow," AIAA Journal of Hydronautics, Vol. 8, No. 3, pp. 100-107 (July 1974).

7. I. H. Abbott, A. E. von Doenhoff and L. S. Stivers, Jr., "Summary of Airfoil Data," NACA Report 824 (1945).

8. G. Kovich and R. J. Steinke, "Performance of Low-Pressure-Ratio Low-Tip-Speed Fan Stage with Blade Tip Solidity of 0.65," NASA TMX-3341 (February 1976).

9. J. A. Koegler, Jr., "A Parametric Wing Design Study for a Modern Laminar Flow Wing," NASA TM 80154 (December 1979).

10. C. O. Wood and F. R. Goldschmied, "Design and Specification Guidelines for Large Draft Fans and Systems," Electric Power Research Institute Report EPRI CS-3431 (January 1984).

11. D. E. Reubush and J. F. Runckel, "Effect of Fineness Ratio on Boattail Drag of Circular-Arc Afterbodies Having Closure Ratios of 0.50 with Jet Exhaust at Mach Numbers up to 1.30," NASA TND-7192 (May 1973).

12. E. E. Larrabee, "Preservation of Wing Leading-Edge Suction at the Plane of Symmetry as a Factor in Wing-Fuselage Design," Proceedings of the NASA-Industry-University General Aviation Drag Reduction Workshop, J. Roskam, Ed., University of Kansas (July 1975), pp. 107-119.